

Lake surface water temperature

Article

Published Version

Carrea, L. ORCID: <https://orcid.org/0000-0002-3280-2767>,
Merchant, C. ORCID: <https://orcid.org/0000-0003-4687-9850>,
Woolway, R. I. ORCID: <https://orcid.org/0000-0003-0498-7968>,
Crétau, J.-F., Dokulil, T. M., Dugan, H., Laas, A.,
Leibensperger, E., Matsuzaki, S.-I., Merio, L. J., Pierson, D.,
Rusanovskaya, O. O., Shimaraeva, S. V., Silow, E. A., Schmid,
M., Timofeyev, M. A. and Verburg, P. (2024) Lake surface
water temperature. Bulletin of the American Meteorological
Society, 105 (8). S33-S35. ISSN 1520-0477 doi:
10.1175/BAMS-D-24-0116.1 (in "State of the Climate in 2023")
Available at <https://centaur.reading.ac.uk/117968/>

It is advisable to refer to the publisher's version if you intend to cite from the work. See [Guidance on citing](#).

To link to this article DOI: <http://dx.doi.org/10.1175/BAMS-D-24-0116.1>

Publisher: American Meteorological Society

All outputs in CentAUR are protected by Intellectual Property Rights law, including copyright law. Copyright and IPR is retained by the creators or other copyright holders. Terms and conditions for use of this material are defined in the [End User Agreement](#).

www.reading.ac.uk/centaur

CentAUR

Central Archive at the University of Reading

Reading's research outputs online

Fig. SB.2.3) and for T_a and T_q individually (Table SB.2.1). The latter both recorded anomalies of 0.6 K relative to the 1991–2020 climatology (see sections 2b1, 2d), but the much lower baseline in T_q translates the 0.6 K anomaly to a relative increase of 2.5%—over an order of magnitude larger than for T (0.21%). This carries through to T_{eq} to some extent, with the relative anomaly in 2023 of 1.2 K representing a rise of 0.38% (Table SB.2.1). As measured by T_{eq} , the climate has therefore departed even further from the reference points of human history.

Although T_{eq} is a complete physical descriptor of atmospheric heating, its unfamiliarity may present a challenge in climate communications, not least because its absolute values (Fig. SB.2.2) and its variability (Fig. SB.2.3) are much higher than for T . However, presenting relative changes as above may be a simple and intuitive solution for overcoming this communication barrier. Such efforts are worth pursuing, as T_{eq} is a key indicator of changes to the atmospheric state that are of critical relevance to society.

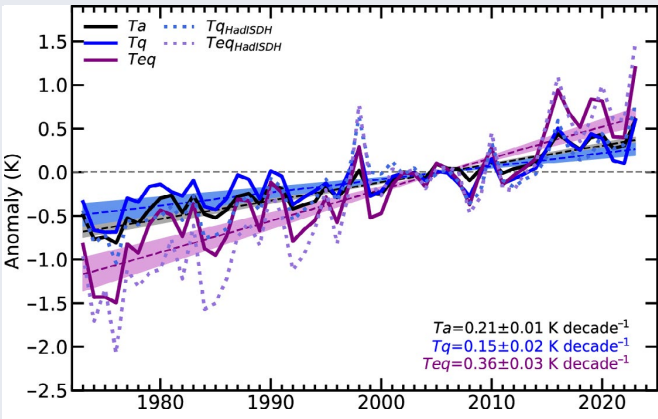


Fig. SB.2.3. 1973–2023 ERA5 and HadISDH trends in global mean air temperature (T_a ; ERA5 only), latent temperature ($T_q = T_{eq} - T_a$), and equivalent temperature (T_{eq}). Trend lines were computed with simple linear regression, and shading spans 95% confidence intervals. The trends presented on the plot are for ERA5, with ± 1 sigma standard error.

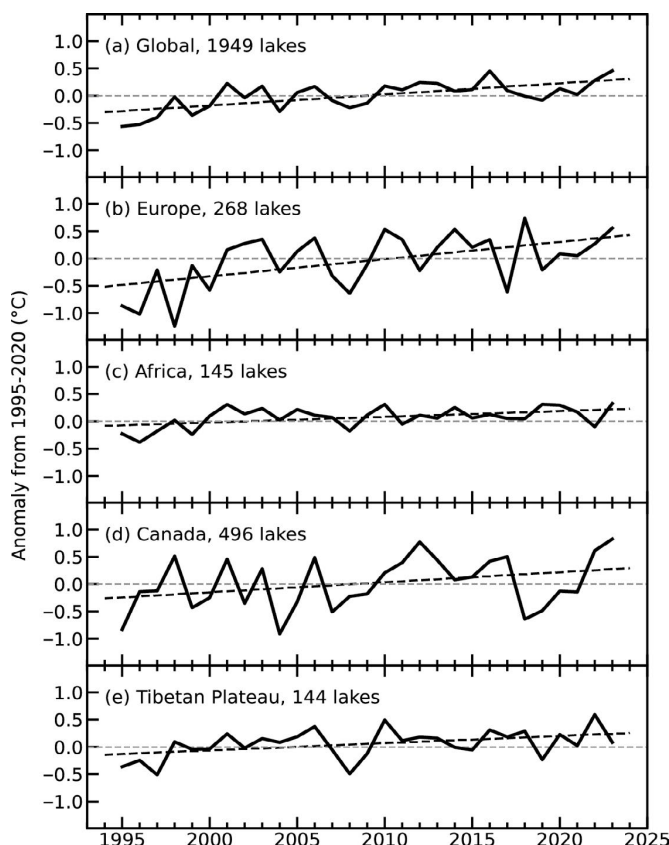
Table SB.2.1. Top-10 years for annual mean values in ERA5 (1973–2023). Note that relative anomalies are computed from the 1991–2020 baseline.									
Rank	Ta year	Ta (K)	Ta (%)	Tq year	Tq (K)	Tq (%)	Teq year	Teq (K)	Teq (%)
1	2023	0.60	0.21	2023	0.60	2.51	2023	1.20	0.38
2	2016	0.44	0.15	2016	0.50	2.12	2016	0.94	0.30
3	2020	0.43	0.15	2019	0.44	1.85	2019	0.84	0.27
4	2019	0.40	0.14	2020	0.38	1.62	2020	0.82	0.26
5	2017	0.34	0.12	2017	0.34	1.41	2017	0.68	0.22
6	2022	0.30	0.10	1998	0.27	1.14	2015	0.52	0.17
7	2021	0.27	0.10	2015	0.27	1.13	2018	0.52	0.17
8	2018	0.26	0.09	2018	0.25	1.07	2021	0.41	0.13
9	2015	0.26	0.09	2010	0.15	0.63	2022	0.40	0.13
10	2010	0.13	0.05	2021	0.13	0.56	1998	0.29	0.09

2. LAKE SURFACE WATER TEMPERATURE

—L. Carrea, C. J. Merchant, R. I. Woolway, J.-F. Crétaux, T. M. Dokulil, H. Dugan, A. Laas, E. Leibensperger, S.-I. Matsuzaki, L. J. Merio, D. Pierson, O. O. Rusanovskaya, S. V. Shimaraeva, E. A. Silow, M. Schmid, M. A. Timofeyev, and P. Verburg

The globally averaged satellite-derived lake surface water temperature (LSWT) anomaly during the 2023 warm season was $+0.46^{\circ}\text{C}$ with respect to the 1995–2020 baseline, the highest since the record began in 1995 (Fig. 2.2a). The mean LSWT trend during 1995–2023 was $0.20 \pm 0.01^{\circ}\text{C decade}^{-1}$, broadly consistent with previous analyses even though the number of lakes analyzed has doubled since 2022 (Woolway et al. 2017, 2018; Carrea et al. 2019, 2020, 2021, 2022a; Fig. 2.2a). The 2023 warm-season anomalies for each lake are shown in Plate 2.1b; of the 1949 studied lakes that were not dry, 79% of these were warmer than average and 21% were colder. For 33 lakes, no anomalies could be computed since they were found to be dry.

Large coherent regions of high LSWT were identified in 2023, with 44% of all observed lakes experiencing LSWT anomalies in excess of $+0.5^{\circ}\text{C}$ (Plate 2.1b). The highest anomalies occurred



in lakes situated in northern Canada, eastern China, Japan, and Europe. Negative LSWT anomalies were consistently observed in Patagonia, Greenland, Alaska, Australia, northern South America, and southeast Asia.

Four regions were studied in more detail: Europe (number of lakes, $n = 268$, Figs. 2.2b, 2.3a), Canada ($n = 496$, Figs. 2.2d, 2.3c), Tibet ($n = 144$, Figs. 2.2e, 2.3d), and Africa ($n = 145$, Figs. 2.2c, 2.3b). In these regions, the warm-season LSWT anomalies are consistent with the corresponding air temperature anomalies, as compiled by NASA's Goddard Institute for Space Studies (GISS; Lenssen et al. 2019; GISTEMP Team 2023), with an average warming trend of $+0.31 \pm 0.03^\circ\text{C decade}^{-1}$ in Europe (Fig. 2.2b) and $+0.18 \pm 0.03^\circ\text{C decade}^{-1}$ in Canada (Fig. 2.2d). In Canada, where the mean LSWT anomaly was $+0.83^\circ\text{C}$ in 2023, 92% of observed lakes had positive anomalies. In Europe, the

Fig. 2.2. Annual time series of satellite-derived warm-season lake surface water temperature anomalies ($^\circ\text{C}$; 1995–2020 base period) from 1995 to 2023 for lakes distributed (a) globally, and regionally in (b) Europe, (c) Africa, (d) Canada, and (e) the Tibetan Plateau.

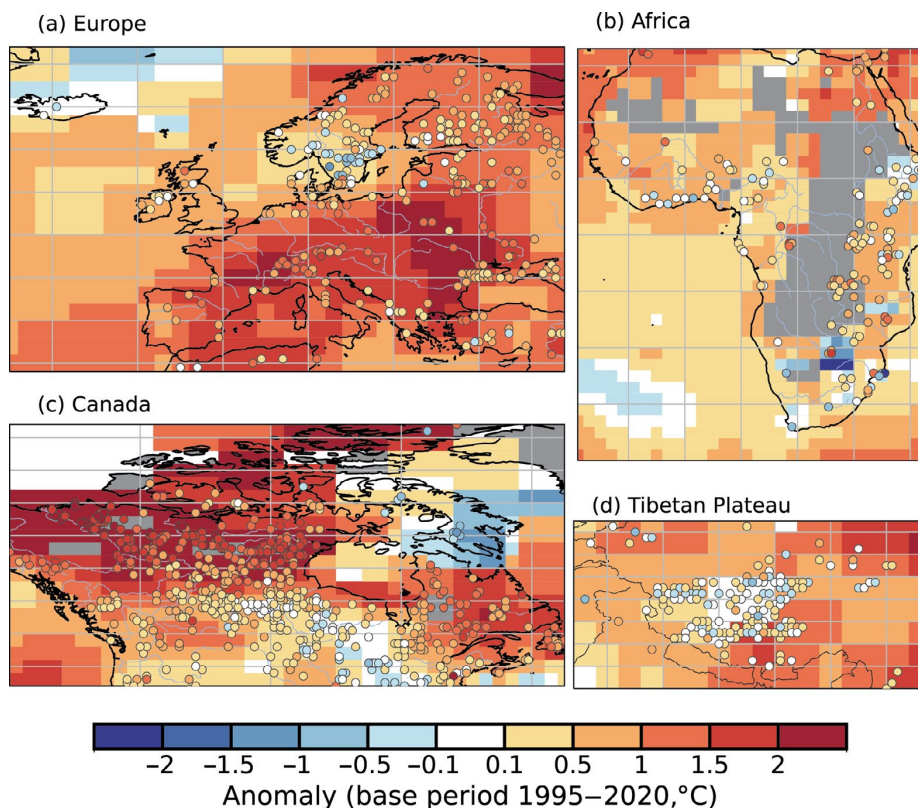


Fig. 2.3. Lake temperature anomalies ($^\circ\text{C}$, colored dots) and 2-m air temperature anomalies ($^\circ\text{C}$) in 2023 for lakes in (a) Europe, (b) Africa, (c) Canada, and (d) the Tibetan Plateau. These values were calculated for the warm season (Jul–Sep in the extratropical Northern Hemisphere; Jan–Mar in the extratropical Southern Hemisphere; Jan–Dec in the tropics) with reference to the 1995–2020 base period.

decade⁻¹ and $+0.10 \pm 0.02^\circ\text{C decade}^{-1}$, respectively (Figs. 2.2c,e). In Africa, 81% of the 145 lakes had positive LSWT anomalies, and the average anomaly in 2023 was $+0.33^\circ\text{C}$. In Tibet, the average 2023 anomaly was $+0.09^\circ\text{C}$, with 70% of the lakes experiencing positive anomalies.

In situ observations of (single-point) warm season temperature anomalies from 38 lakes are shown in Fig 2.4, 23 of which have measurements for the year 2023, with an average of $+0.78^\circ\text{C}$. The anomalies calculated here differ from those derived from satellite data, which represent lake-wide averages. Five lakes experienced negative anomalies (average of -0.76°C) and 18 lakes had positive anomalies (average of $+1.21^\circ\text{C}$) in 2023. The time series in Fig. 2.4 clearly show that lakes are warming.

The period 1995–2020 is used as a baseline for both in situ (unless no data were available) and satellite temperatures to compute anomalies. The warm-season averages for midlatitude lakes were computed for summers (July–September in the Northern Hemisphere and January–March in the Southern Hemisphere), and January–December averages are presented for tropical lakes (within 23.5° of the equator).

Lake surface water temperature time series were derived from the European Space Agency Climate Change Initiative (ESA CCI) LAKES/Copernicus Climate Change Service (C3S) /Earth Observation Climate Information Service (EOCIS) climate data record (Carrea et al. 2022b, 2023). The LSWT time series has been derived using ATSR2, AATSR, MODIS, AVHRR and SLSTR sensors. For 2023, satellite observations from SLSTR on Sentinel3A and 3B were used. The retrieval method of MacCallum and Merchant (2012) was applied on image pixels filled with water according to both the inland water dataset of Carrea et al. (2015) and a reflectance-based water detection scheme (Carrea et al. 2023).

The satellite-derived LSWT data are spatial averages for each of a total of 1949 lakes. The satellite-derived LSWT data were validated with in situ measurements with an average satellite-minus-in situ temperature difference of less than 0.5°C and standard deviation (robust) of less than 0.7°C (Carrea et al. 2023). Lake-wide average surface temperatures have been shown to give a more representative picture of LSWT responses to climate change compared to single-point measurements (Woolway and Merchant 2018).

The average surface air temperature was calculated from GHCN v4 (250-km smoothing radius) data of the NASA GISS surface temperature analysis (Lenssen et al. 2019; GISTEMP Team 2024).

3. NIGHT MARINE AIR TEMPERATURE

—R. C. Cornes and R. Junod

Two night marine air temperature (NMAT) datasets are routinely updated and used for analysis in this section: UAHNMAT (Junod and Christy 2020) and CLASSnmat (Cornes et al. 2020). These datasets are evaluated in combination with the HadSST4 dataset (Kennedy et al. 2019). Since these datasets are not spatially interpolated, they each have slightly different spatial coverage. In this evaluation the data have been masked to allow comparisons to be made over the common coverage areas, and to the common period of 1900–2023. NMAT and sea-surface temperature

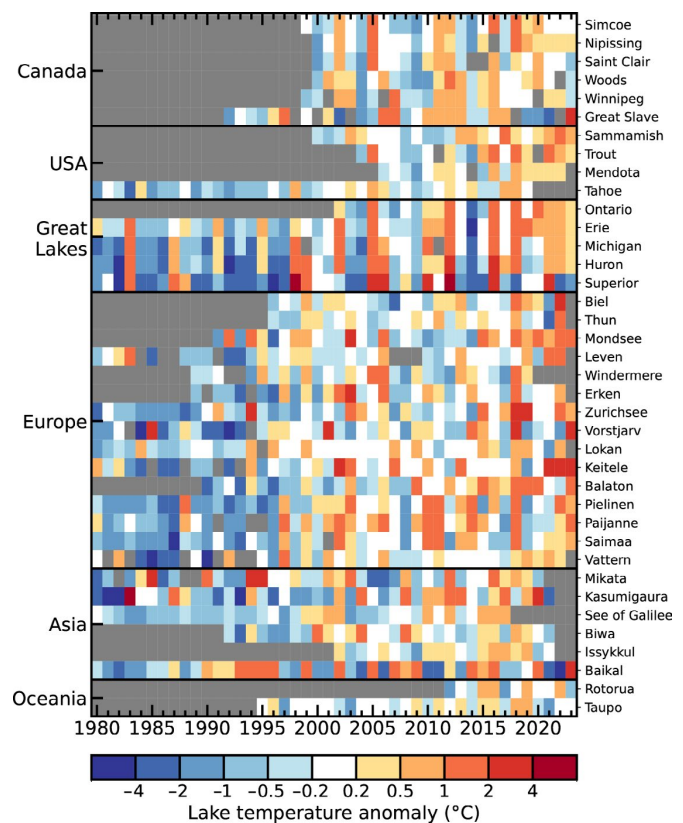


Fig. 2.4. In situ lake surface water temperature observations from 38 globally distributed lakes, showing the annually averaged warm season (Jul–Sep in the Northern Hemisphere; Jan–Mar in the Southern Hemisphere) anomalies ($^\circ\text{C}$; 1995–2020 base period or the available base period).